CORE MELT RETENTION CAPABILITY OF CANDU REACTORS

A.P. Muzumdar, P.M. Mathew
Atomic Energy of Canada Limited, Canada

J.T. Rogers and M.L. Lamari
Carleton University, Canada

ABSTRACT

A simple molten pool heat transfer model has been set up for the CANDU reactor to perform sensitivity studies and understand the effect of differences from a LWR-like geometry. By varying important material properties of CANDU corium over the predicted range, the effect on vessel steel temperatures and heat flux to the surrounding water inherent in the CANDU design is determined. It is concluded that the melt is retained in the calandria vessel with a large margin to dryout. Comparison with the LWR-like geometry shows that steel temperatures are much higher due to the thicker vessel wall in a LWR, otherwise the results are similar, assuming external cooling is available. In both geometries, a large fraction of the core power is radiated upwards. The results of the CANDU analysis are confirmed with a more detailed transient debris melting model.

INTRODUCTION

In accident sequences in a CANDU reactor in which the fuel heat is not removed by normal or emergency coolant in the heat transport system, the separately cooled moderator provides an effective heat sink which ensures that no gross melting of the fuel occurs and pressure-tube integrity is maintained (Muzumdar et al, 1983, Sanderson et al, 1996). In certain scenarios, however, there is a low probability that the moderator heat sink could be ineffective in these types of accidents. Various studies, based on early work by Rogers, 1984, have indicated that, although core disassembly would occur as the moderator boiled off, the core debris, whether solid or molten, would be contained within the calandria as long as it remained cooled by the shield-tank water. Boil-off of shield-tank water could eventually lead to calandria vessel failure, typically at times greater than 24 hours after initiation of the accident, when the decay power level has decreased to about 0.5%, allowing considerable time for operator intervention. A good summary and background to this topic may be found in Meneley et al, 1996. A summary of related CANDU severe core damage research aspects is given in Simpson et al, 1996.

External cooling is a standard design feature in CANDU reactors. It is being considered as an accident management system via external flooding for other reactor types such as LWRs (Kymalainen et al, 1997, NEA/CSNI, 1994, Henry et al, 1993). Due to its direct relevance, Canada is a participant in the OECD/NEA/Russia-sponsored RASPLAV program, which is aimed at studying the thermal-hydraulics and materials interaction behaviour of an externally cooled molten pool using real PWR corium at reasonably large scale (Speis and Asmolov, 1995).

This paper presents a summary of some recent parametric calculations which have been performed to investigate the eventual quasi-steady state molten pool behaviour of the debris, particularly the effect of uncertainties in the corium thermophysical properties on peak temperatures and heat flux to the shield tank water. Since the geometry of the CANDU reactor is quite different to the LWR, similar calculations are performed for an equivalent LWR-like geometry, to understand the effect, if any, of the differences between the two geometries. Note that the analysis presented is not a severe core damage analysis, per se, so there is no attempt to capture all phenomena, but is primarily a study of the effect of geometry on heat transfer, using a simple core melt model. This is important in order to extrapolate the RASPLAV results, which are essentially obtained using PWR geometry and corium, to CANDU geometry and corium. Also included for comparison is some recent work on modeling the transient debris melting which precedes the formation of the molten pool. Further details may be found in Muzumdar et al, 1998, Rogers and Lamari, 1997.

MOLTEN CORIUM PROPERTIES

Table 1 shows the thermo-physical properties of CANDU and PWR molten corium mixtures for various Zr oxidation levels. The power densities shown are typical of CANDU and PWR. The composition of CANDU corium was calculated from the original materials inventory of a CANDU-6, neglecting minor alloying components such as Nb and Sn and control rod materials.

Table 1 Molten Corium Properties

CORIUM Type	CANDU-6 CORIUM		TYPICAL PWR CORIUM	
Power Density @ 1% power (MW th/Mg)	0.14		0.25	
% Zr Oxidized	25	100	22	100
Composition (wt%)	68.5% UO_2 9.8% ZrO_2 21.7% Zr	63.6% UO_2 36.4% ZrO_2	81.5% UO_2 5.0% ZrO_2 13.5% Zr	77.8% UO_2 22.2% ZrO_2
Solidus Temperature (K)	2173	2840	2173	2800
Liquidus Temperature (K)	2673	2840	2673	2830
Specific Heat (J $kg^{-1}K^{-1}$)	530	590	528	590
Thermal Conductivity (W $m^{-1}K^{-1}$)	20.0	4.6	11.0	4.6
Kinematic Viscosity (m^2s^{-1})	$9.0\ 10^{-7}$	$8.5\ 10^{-7}$	$7.3\ 10^{-7}$	$9.5\ 10^{-7}$
Density (kg m^{-3})	7560	7300	8300	7860
Vol. Expansion Coefficient (K^{-1})	$8.0\ 10^{-5}$	$9.3\ 10^{-5}$	$8.7\ 10^{-5}$	$9.6\ 10^{-5}$

The solidus and liquidus temperatures were estimated from the U-Zr-O ternary phase diagram (MATPRO, 1990). The other properties of CANDU corium were calculated from the component properties of UO_2, ZrO_2 and Zr. In the calculations the mixture properties were calculated using a model based on averaging the properties of the three components, according to their mole fraction in the respective mixture. Application of this method to the selected corium compositions for which thermo-physical data have been measured shows satisfactory agreement between this calculational method and the available experimental data. It should be noted that this method assumes that the melt is homogeneous and that no melt separation occurs at the high temperatures. The properties of PWR-type corium were based on preliminary RASPLAV data.

MOLTEN POOL SENSITIVITY STUDIES

A lumped parameter model was set up to describe the heat balance of a molten corium pool contained within the cylindrical calandria vessel of the CANDU reactor (Figures 1 and 2). Heat transfer modes included (1) downward, horizontal, and upward convection from the molten pool, conduction through the corium crust, (2) radiation from the top surface to the side and upper steel walls, based on view factors determined separately, and (3) conduction through the steel to the water in the shield tank. The convective heat transfer correlations were based on those by Mayinger (down), and Steinberger and Reineke (up, horizontal) as reported by Kymalainen et al,1994. A vertical angle of 45^o was arbitrarily used to differentiate between the downward and horizontal heat flux, although in practice the melt pool height was low enough that the downward heat flux always dominated. Note that the pool "sink" temperature in the correlations is the molten corium/crust interface temperature T_{int} (defined as the average of the solidus and liquidus temperatures, since in reality a "mushy" region is likely to form in the two-phase region), and the characteristic length is taken as the pool height H. The steel outer surface temperature was maintained constant at 400 K based on the results which indicate that nucleate boiling would occur as long as water is present on the outside. For a given geometry, pool height, and power density, the model returns the various directional heat fluxes, the peak melt temperature, and the crust and steel temperatures around the vessel. Thinning of the steel wall due to melting is inherently included, although in practice, the power density used here does not result in any steel melting. The heat balance model was similarly set up for the LWR-like geometry shown on the right side of Figure 1.

FIGURE 1

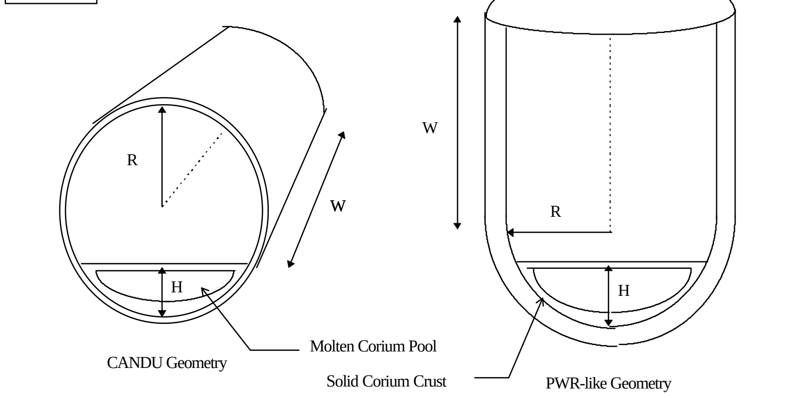

NOTE: Both above geometries are assumed to be well cooled on the outside by 100^{o}C saturated water

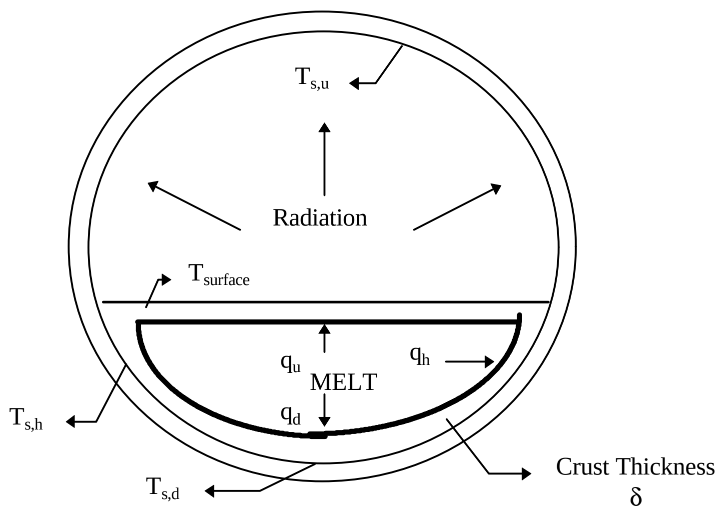

FIGURE 2 CANDU Cross-section & Heat Transfer Directions

Table 2 Sensitivity Study Parameters

	Reference Value Assumed	Sensitivity Range
Molten Corium/Crust Interface Temperature T_{int} (K)	2630 (Average of solidus and liquidus temperatures)	±10%
Melt Specific Heat C_p ($J\ kg^{-1}K^{-1}$)	560	±10%
Melt Thermal Conductivity k_m ($W\ m^{-1}K^{-1}$)	12.3	±75%
Melt Kinematic Viscosity ν (m^2s^{-1})	$8.5\ 10^{-7}$	±10%
Melt Density ρ ($kg\ m^{-3}$)	7430	±10%
Melt Vol. Expansion Coefficient β (K^{-1})	$8.6\ 10^{-5}$	±10%
Crust Thermal Conductivity k_c ($W\ m^{-1}K^{-1}$)	8.0	±50%
Crust Emissivity ε_c	0.6	±50%
Steel Thermal Conductivity k_s ($W\ m^{-1}K^{-1}$)	40.0	Not varied
Steel Emissivity ε_s	0.3	Not varied
Steel Outer Surface Temperature T_o (K)	400	Not varied

The reference thermo-physical properties and ± range employed in the sensitivity study are shown in Table 2. The sensitivity study approximately covers the range of melt properties shown in Table 1 for low to fully oxidized CANDU and LWR corium. In particular, the melt thermal conductivity k_m has a ±75% range, and is known to be important. Since the crust thermal conductivity and emissivity are uncertain, reference values were used with a large uncertainty of ±50%. The steel properties were not varied as these are known more accurately.

The reference CANDU-6 vessel geometry, corium mass, volume, and power density parameters, are shown in the second column of Table 3. The third column lists the parameters used for the "equivalent" LWR-like geometry shown in Figure 1. Note that the (normally low pressure) calandria vessel wall thickness in

Table 3 Reference Parameters (see Figures 1 and 2)

	CANDU-6 Geometry	LWR-like Geometry
Internal Vessel Radius R (m)	3.77	3.77
Length of Cylinder W (m)	6	6
Steel Wall Thickness (cm)	3.1	10 (spherical lower head) 20 (cylindrical section)
Height H of Corium (m)	1.0	1.43
Volume of Corium (m^3)	21.1	21.1
Mass of Corium (Mg)	157	157
Nominal Full Power (MW Thermal)	2180	2180
Power Density (Thermal) @ 1% Decay Power	1.03 (MW/m^3) 0.14 (MW/Mg)	1.03 (MW/m^3) 0.14 (MW/Mg)
Radiation Heat Transfer Area (m^2)	30.7	27.4
Conduction Heat Transfer Area (m^2)	33.7	33.9
External Steel Temperature (K)	400	400
Ra Number @ 1% Decay Power	$2.9\ 10^{13}$	$1.7\ 10^{14}$

CANDU is only 3.1 cm, compared to the much thicker LWR vessel. For the purposes of this study, the LWR-like vessel is assumed to be 10 cm thick in the spherical lower head, and 20 cm thick in the upper cylindrical section.

Note also that the CANDU and LWR-like vessels are assumed to have identical internal radius R; length of the cylindrical section W; mass, volume, and power density of corium (although PWRs typically have much higher power density as shown in Table 1). The pool height H is 1.0 m for CANDU-6 (based on results presented later), versus about 1.4 m for the LWR-like geometry, due to the horizontal cylindrical vessel design of CANDU. At 1% decay power, this results in a lower Rayleigh number (Ra) in CANDU of 2.9 10^{13} compared to 1.7 10^{14} for the LWR-like reactor (since Ra ~H^5). Since convective heat transfer increases with Ra number, one of the objectives of the RASPLAV program is to obtain data for Ra between 10^{15} and 10^{16} so that it is more relevant to current LWRs. It is clear that the existing corium data at around Ra ≤ 10^{13} is applicable to CANDU for decay power ≤ 1%.

It is interesting that the total conduction heat transfer area (contact area with the steel wall) for the two geometries in Figure 1 are almost identical, but the radiation heat transfer area (top surface) is about 10% greater in CANDU. This, again, is due to the horizontal cylindrical geometry. Note that the geometric parameters listed in Table 3 for the LWR-like reactor closely resemble actual BWRs. In the case of PWRs, thermal power and power density, which tend to be much higher compared to the CANDU-6 reactor, all else being equal.

Table 4 shows the results of the sensitivity study for 0.5% and 1% decay power for the main variables of interest. As expected, the results are insensitive to C_p, ν, ρ and β. The crust emissivity ε_c affects only the surface temperature and upper crust thickness. The crust conductivity k_c directly affects only the crust thicknesses. The interface temperature T_{int} affects only the pool temperature T_{max}, and has a large effect on the upper crust thickness. *The melt thermal conductivity k_m is the only parameter that significantly affects all variables, in particular, the heat fluxes and steel temperatures. Even then, the effects are not large; e.g., ±75% in k_c results in only +5.1% and -11.5%, respectively, in the downward heat flux q_d.*

Table 4 Results of Sensitivity Study

Parameter	Reference @		% Sensitivity to Effect of…				
	1%,	0.5%	$k_m \pm 75\%$	$T_{int} \pm 10\%$	$k_c \pm 50\%$	$\varepsilon_c \pm 50\%$	C_p[1] ± 10%
Maximum Melt Temp. T_{max} (K)	2729	2688	−1.0 +4.3	+9.5 −9.5	0	0	−0.1 +0.1
Crust Surface Temp. $T_{surface}$ (K)	2290	1922	−0.3 +0.7	0	0	−5.6 +12.7	0
Upper Steel Temp. $T_{s,u}$ (K)	597	498	−0.4 +0.9	0	0	0	0
Lower Steel Temp. $T_{s,d}$ (K)	496	449	+1.0 −2.2	0	0	0	−0.1 +0.1
Side Steel Temp. $T_{s,h}$ (K)	690	548	+1.6 −3.8	0	0	0	−0.1 +0.2
Upward Heat Flux q_u (kW m^{-2})	575	285	−1.2 +2.7	0	0	0	+0.1 −0.1
Downward Heat Flux q_d (kW m^{-2})	123	64	+5.1 −11.5	0	0	0	−0.4 +0.5
Horizontal Heat Flux q_h (kW m^{-2})	374	191	+3.9 −9.0	0	0	0	−0.3 +0.4
Power Radiated Upwards P_{rad} (%)	80.9	80.3	−1.2 +2.7	0	0	0	+0.1 −0.1
Upper Crust Thickness δ_u (cm)	0.48	2.00	+3.3 −7.1	+76.4 −76.4	+50.0 −50.0	+37.5 −85.6	−0.3 +0.3
Lower Crust Thickness δ_d (cm)	13.8	27.5	−5.1 +13.6	+12.2 −12.2	+50.0 −50.0	0	+0.5 −0.5
			NOTE: All values shown above are in % of the Reference Value @ 1% decay power (the values at 0.5% decay power are similar).				

[1] The sensitivity results in this column also apply to the melt kinematic viscosity, volumetric expansion coefficient, and density, due to the linear dependence of the Ra number on these parameters.

Figure 3 shows corium and steel temperatures versus decay power for the CANDU and LWR-like geometries. With the exception of the steel temperatures, there is little difference between the two (e.g., T_{max} is almost identical). The thicker steel wall in the LWR-like case results in much higher steel temperatures compared to CANDU. High steel temperatures can be a potential concern with regard to eutectic formation, *even when water cooling is assumed on the outside*.

FIG 3 Corium and Steel Temperatures

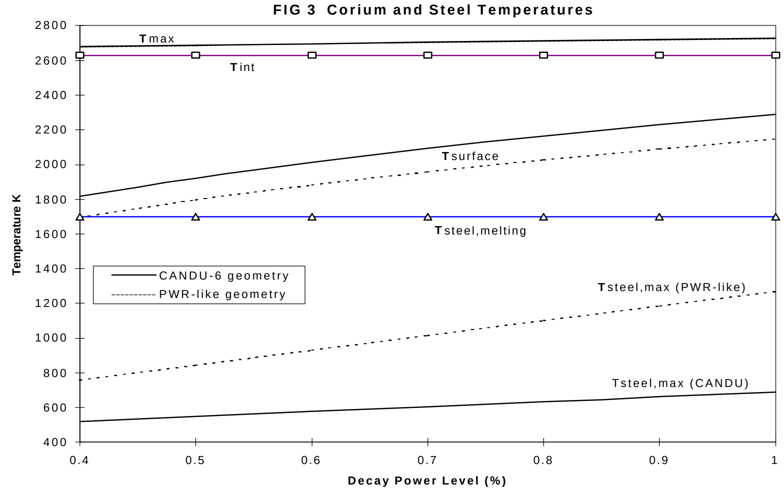

Figure 4 shows that the core power radiated upwards by the crust surface is about 80% for CANDU, versus 72% for the LWR case. The difference is mainly due to the greater heat removed horizontally in the LWR case (larger pool height).

FIG 4 Power Radiated from Upper Surface

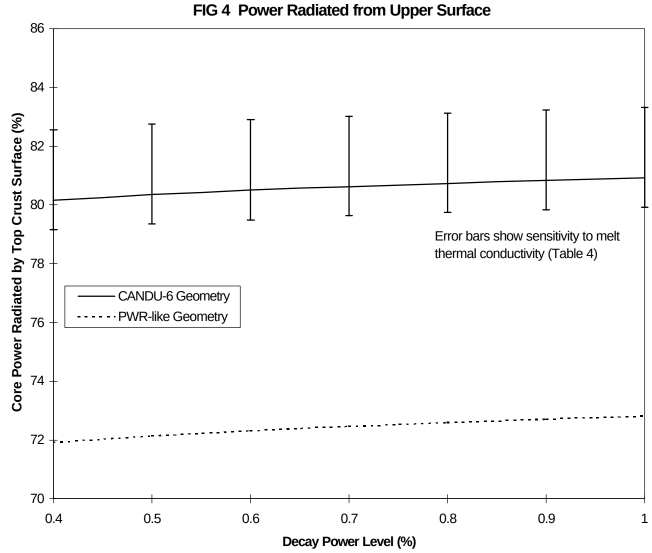

Figure 5 shows the downward heat flux and the maximum critical heat flux ratio (these results are almost identical for the two geometries). The minimum CHF is taken as 300 kWm^{-2} based on NEA/CSNI, 1994. No dryout of the steel vessel is expected over the power range examined. Hence, the assumption of external nucleate boiling is valid. In the following section, a comparison of the simple model described above, and a more detailed transient debris melting model, is presented to confirm the validity of the former.

FIG 5 Downward heat flux

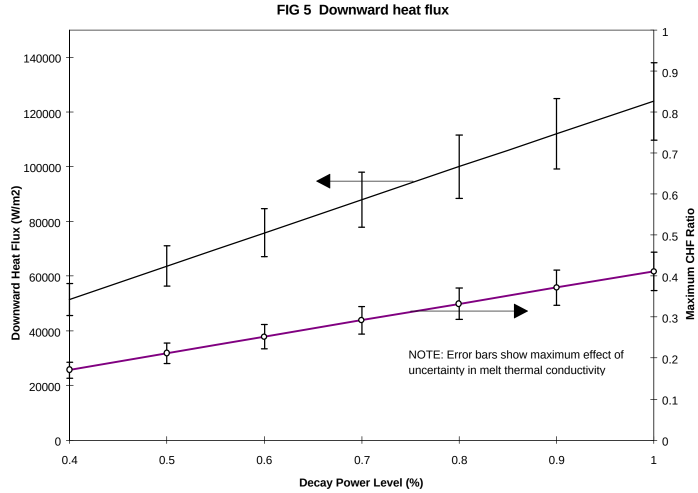

RESULTS OF TRANSIENT DEBRIS MELTING MODEL

The DEBRIS.MLT model has been developed as an extension of the transient, one-dimensional, explicit finite-difference model DEBRIS.2, incorporating certain modified elements of the corium molten pool model MOLPOOL (similar to that described above) as well as an improved model for debris-bed thermal conductivity (Rogers and Lamari, 1997). It is assumed that melting of the debris occurs at a constant temperature of 2973 K (2700^{o}C)[2], during which the fraction of molten material at a node is calculated by a heat balance which accounts for decay heat and any heat generated by the zirconium-steam reaction, as well as heat flow rate to and from the node. The heat flow rates are based on the effective conductivities of a mixture of solid and molten debris in the upward and downward directions, calculated as the weighted sum of the effective thermal conductivities of the porous solid debris and of the molten corium for the adjacent nodes in question. The effective thermal conductivity of the molten corium allows for natural convection of the corium by multiplying its actual thermal conductivity by an appropriate Nusselt number for the node conditions and for heat flow in the appropriate direction. The distance between nodes is treated as a variable that may change with node position and time. This treatment allows for changes in debris geometry after melting begins. As melting progresses, molten corium fills the voids in the debris bed and the melting of debris also causes re-arrangement (collapse) of remaining solid material. A simple model for the geometry change during melting is assumed in which the porosity at a node and the distance between nodes are simple functions of the molten fraction at the node.

Once all the material in a node is molten, the model allows for a subsequent temperature rise, as well as mixing between completely molten nodes. The latter uses a method of weighting the temperatures of adjacent nodes by a factor determined from a comparison of the results obtained at long times with those of the quasi-steady-state model MOLPOOL. As the decay heat source decreases with time and all the zirconium is consumed, the node temperatures reach maximum values and then begin to decrease. As cooling occurs, temperatures eventually reach a value at which the corium begins to re-solidify.

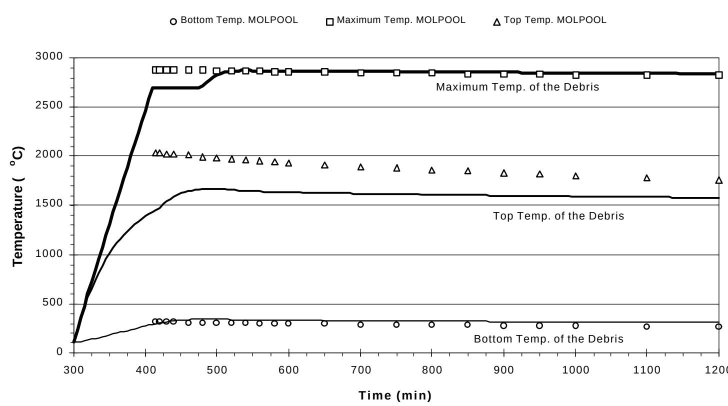

Figure 6: Comparison of Selected Temperatures Predicted by DEBRIS.MLT and MOLPOOL. Reference Conditions.

Figure 6 shows the temperature histories at different points in the debris and corium for the reference conditions, which assume that debris heatup begins at 5 hours (or about 1% decay power). The solid debris heats up until the melting point at the hottest node is reached at about 415 minutes. The maximum temperature, which occurs at a node at about the mid-point of the debris, remains at the melting point, 2700^{o}C, until all the debris at this node has melted. This occurs at about 480 minutes, so that complete melting at this node takes about 65 minutes. Superheating of the corium at this node then begins with the temperature of the corium reaching a maximum of about 2880^{o}C (3153 K) at about 540 minutes. This result is very consistent with the value of T_{max} in Table 4, when account is taken of the sensitivity to the higher T_{int} (2973 K versus 2630 K) and lower k_m (3.6 versus 12.3 W $m^{-1}K^{-1}$) assumed in the DEBRIS.MLT model reference

[2] 2973 K is approximately the melting temperature of ZrO_2. This is higher than the solidification temperature of the molten corium mixture, or equivalently, the interface temperature T_{int} = 2630 K in Table 2. The debris melt model has assumed that the melting and solidification temperatures are equal.

case.

Figure 7 shows the variation with time of the total depth of the debris bed during bed heat-up, melting transient and corium pool development. After melting starts at about 415 minutes, the total height begins to decrease from the initial 1.65 m as molten material starts to fill the voids, and the solid debris collapses. The total depth, including top and bottom "crusts" and the molten pool, reaches a minimum of about 1.0 m (cf. H value in Table 3) at about 520 minutes and remains constant after that time. Figure 8 shows the heat fluxes to the shield-tank water from the calandria wall. In particular, the downward heat flux reaches a peak of about 115 kWm^{-2}. This result agrees with Figure 5, confirming that no dryout of the vessel is expected..

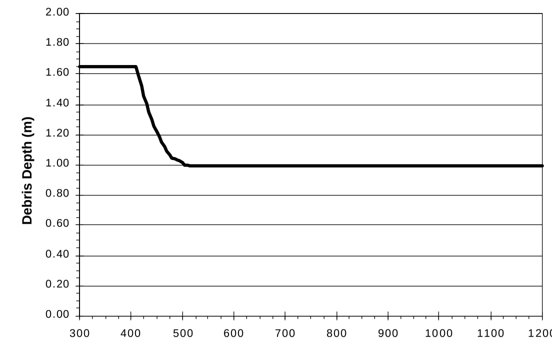

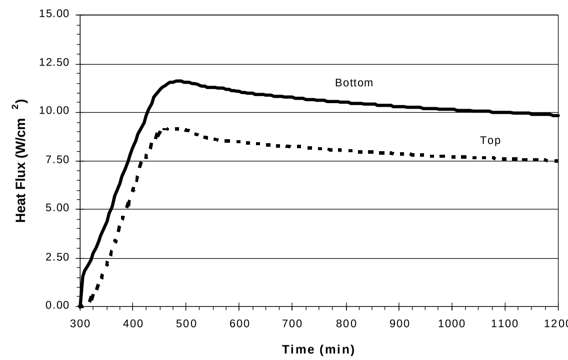

Figure 8: Heat Flux to Shield Tank Water

Sensitivity studies have been performed using DEBRIS.MLT which confirm the results in Table 4. In addition, the results have been found to be insensitive to the debris porosity and pore size, and to heat addition by the Zr-steam reaction in the debris (Rogers and Lamari, 1997).

CONCLUSIONS

A simple molten pool heat transfer model was set up in order to perform sensitivity studies, and to understand the effect of differences between a CANDU geometry and a LWR-like geometry, assuming that both are externally cooled by water. By varying important material properties over the range predicted for CANDU and PWR corium, it was determined that the melt thermal conductivity is the most sensitive variable for the parameters of interest such as the steel temperatures and the heat flux to the surrounding water, although the relative effects are small.

The CANDU and LWR-like geometries give similar results for the same core power density, with the exception of the steel temperatures, which are much higher in the LWR-like reactor due to the thicker vessel wall. The CANDU design does not require a thick wall pressure vessel.

The Rayleigh number Ra, which governs natural convective heat transfer from the melt to the vessels walls, is relatively low in CANDU ($<2.9\ 10^{13}$) compared to LWR. Hence, existing correlations up to Ra of 10^{13} for corium melts are expected to apply with confidence.

There is a large margin to dryout of the CANDU calandria vessel, allowing melt retention via external cooling inherent in the CANDU design. The potential for corium phase separation is being addressed through participation in the RASPLAV program. The maximum steel vessel temperatures are low due to the relatively thin calandria vessel wall, so that melting of the steel walls is not an issue.

The results obtained with the simple molten pool heat transfer model are confirmed with the more detailed transient debris melting model DEBRIS.MLT.

REFERENCES

Henry, R.E. et al, “Cooling of Core Debris Within the Reactor Pressure Vessel Lower Head”, *Nuclear*

Technology, **101**, March 1993.

Kymalainen, O. et al, “In-Vessel Retention of Corium at the Loviisa Plant”, *Nuclear Engineering and Design*, **169** (1997), 109-130.

Kymalainen, O. et al, “Heat Flux Distribution From a Volumetrically Heated Pool With High Rayleigh Number”, *Nuclear Engineering and Design*, **149** (1994), 401-408.

MATPRO - A Library of Materials Properties for Light Water Reactor Accident Analysis, NUREG/CR-5273, EGG-2555, Vol.4, 1990.

Meneley, D.A., C. Blahnik, J.T. Rogers, V.G. Snell and S. Nijhawan, “Coolability of Severely Degraded CANDU Cores”, AECL-11110, July, 1995, Revised January, 1996.

Muzumdar, A.P. et al, "Fuel Channel Behaviour During Accidents with Degraded Cooling in CANDU Reactors", IAEA Specialists' Meeting on Water Reactor Fuel Safety and Fission Product Release in Off-Normal and Accident Conditions, Riso National Laboratory, Denmark, May 16-20, 1983.

Muzumdar, A.P., J.T. Rogers, P.M. Mathew and M. Lamari, “Analysis of Core Melt Retention Capability of CANDU Reactors”, paper to be presented at the 6th International. Conference on Nuclear Engineering (ICONE-6), May 10-15, 1998, San Diego, California, U.S.A.

NEA/CSNI (OECD/NEA) Report by a Group of Experts, “Core Debris Cooling with Flooded Vessel or Core Catcher”, NEA/CSNI/R(94)32, Sept.1994.

Rogers, J.T. and M. Lamari, “Transient Melting and Re-Solidification of CANDU Core Debris in Severe Accidents”, Proc.20th Canadian Nuclear Society Simulation Symposium, Niagara-on-the-Lake, Ontario, Canada, Sept. 7-9, 1997.

Rogers, J.T., “Thermal and Hydraulic Behavior of CANDU Cores Under Sever accident Conditions - Final Report”, Vol. 1 & 2, Atomic Energy Control Board INFO-0136, June 1984.

Sanderson, D.B., R.G. Moyer and R. Dutton, “Effectiveness of the Moderator as a Heat Sink During a Loss-of-Coolant Accident in a CANDU-PHWR Reactor”, *Heat and Mass Transfer in Severe Nuclear Reactor Accidents*, J.T. Rogers, Editor, Begell House Inc., New York (1996).

Simpson, L..A., P.M. Mathew, A.P. Muzumdar and D.B. Sanderson, “Severe Accident Phenomena and Research for CANDU Reactors”, 10th Pacific Basin Nuclear Conference, Kobe, Japan, 20-25 October, 1996.

Speis, T.P. and V. Asmolov, “RASPLAV: Refining RPV Integrity Strategies for Accident Management”, *Nuclear Europe Worldscan*, **15** (9-10), 1995.